Scholars Journal of Physics, Mathematics and Statistics **ISSN 2393-8056 (Print)**
Abbreviated Key Title: Sch. J. Phys. Math. Stat. **ISSN 2393-8064 (Online)**

(An International Publisher for Academic and Scientific Resources)

Mechanochemical Synthesis of Antimony Selenide (Sb_2Se_3) by Dry Milling: Structural Properties

Sifawa A[1*], Abdullahi S[2]
[1]Department of Physics, Sokoto State University Sokoto, Nigeria
[2]Department of Physics, Usmanu Danfodiyo University Sokoto, Nigeria

***Corresponding author**
Sifawa A

Article History
Received: 12.10.2018
Accepted: 23.10.2018
Published: 30.10.2018

DOI:
10.21276/sjpms.2018.5.5.3

Abstract: Sb_2Se_3 is a very promising photovoltaic material because of its attractive material, optical and electrical properties. In this paper, Sb_2Se_3 has been synthesized by dry ball milling from Sb and Se powders. It has been found out that a single phase Sb_2Se_3 can be achieved after six hours of dry milling under argon atmosphere. XRD, Raman, FE-SEM and EDAX analyses confirmed the existence of the single phase. The present study opens a new avenue to low-cost, large-scale synthesis of high-quality semiconductor with technological applications in solar energy conversion and also for a wide range of optical devices.
Keywords: Ball milling, Sb_2Se_3, Dry milling, Synthesis, XRD.

INTRODUCTION

Metal selenides have attracted considerable attention due to their interesting properties and potential applications in many areas of Chemistry and Physics. Specifically, Antimony selenide (Sb_2Se_3) belongs to V–VI family [1] with orthorhombic crystal structure, in which each Sb- atom and each Se-atom is bound to three atoms of the opposite kind that are then held together in the crystal by weak secondary bonds. Compound Sb_2Se_3 belongs to the space group *Pnma* 62. With a melting point of 500^0C, the elemental storage of Sb and Se in earth crust stands at 0.2 and 0.05 ppm respectively. The storage of Sb is higher than that competitors such as Indium (0.049 ppm) and Tellurium (0.005 ppm) [2].

It finds applications as a thermoelectric and also as a pristine material for memory switching. It is also used for optical coatings in thermophotovoltaics, thermoelectrics, photodetectors, topological insulators as well as anode material in sodium ion batteries [3]. Its high refractive index and optical band gap (being both direct and indirect) transitions ranges from 1 to 1.2 eV [4]. In comparison to the most popular inorganic compound absorbers such CIGS and CZTSSe, antimony selenide is simple in terms of binary constituents and thereby reduces the chances of formation of secondary phases. The process of milling which originates from mechanical alloying (MA), is a significant unit operation in many fields such as chemistry, pharmacy, mineral processing, and materials science. Many types of mills are employed in these fields and are ideally suited for wet or dry grinding processes, size reduction and dispersion, and deflocculation in solid–liquid systems. Ball milling on the other hand is a process where by a powder mixture placed in the ball mill is subjected to high-energy collision from the balls. This process was developed by Benjamin and his co-workers at the International Nickel Company in the late of 1960. It was found that this method, termed mechanical alloying, could successfully produce fine, uniform dispersions of oxide particles.

Antimony selenide (Sb_2Se_3) has been synthesized by different methods such as single source precursor [5], hydrothermal reaction [6], physical vapor-liquid-solid (VLS) [7], microwave-activated solvothermal reaction [8], solid state synthesis and ball milling [3, 9], chemical vapor transport reaction [10], rolling mechanism [11], simple colloidal process [12] and CBD [13-14].

The main purpose of this report is to provide information on direct synthesis of Antimony selenide at room temperature by dry ball milling process.

EXPERIMENTAL DETAILS

Elemental powders of Antimony (99.99%) and selenide (99.99%) in stoichiometry ratio of 2:3 were put in the milling jar (volume 250 ml) containing 25 grinding balls of 10 mm each. The jar was then placed in the planetary ball mill Fristsch Pulverisette P-6. The ball to powder ratio was kept constant at 15:1 throughout the grinding process. The rotation speed was constantly maintained at 500 RPM under argon atmosphere. The whole process lasted for 6 hours with sample being collected after every 60 minutes. The Sb_2Se_3 phase formation was detected by high-resolution X-ray diffraction (X-pert pro diffractometer)

operated at 40 kV and 30 mA, Raman scattering spectroscope (Reinshaw invia Raman Microscope) with an Olympus microscope equipped with a 100X magnification lens and in the backscattering configuration. The excitation source was a green Argon ion laser operating at 532 nm and 220 mW output powers. The morphology and the elemental composition of the samples was inspected by Field Emission Scanning Electron Microscope (FET Quanta USA) operated at 30 kV at a magnification of 10,000X. The Energy Dispersive X-ray analysis (EDAX) was recorded in the binding energy region of 0 to 16 KeV.

RESULTS AND DISCUSSION

Figure 1 shows the XRD patterns of the as-milled Sb_2Se_3 by dry milling. It can be seen from the figure that at 1 hour of milling, Sb_2Se_3 started forming with Sb being the main phase. The only low intensity peak that can be attributed to elemental Se was located at $2\theta = 24^0$. In this figure, the most dominant peak belongs to Sb at $2\theta = 28^0$. At 3 hours of milling, elemental Sb dominates forming as indicated by the peaks. Peaks belonging to both Sb increased in intensity as compared to those milled for 1 hour. This increase in intensity is attributed to good crystallinity of the samples [15-16]. At 6 hours of milling, single phase of Sb_2Se_3 (2 1 2) was formed at $2\theta = 31.47^0$. The full width at half maximum (FWHM) and the crystallite size was determined at 0.44427 and 184.92 respectively. Narrow peaks seen are attributed large grain size [13]. Strong peaks on the other hand suggests preferential growth along the prepared plane [17]. All the peaks in the powder pattern were indexed with reference to the available XRD pattern for Sb_2Se_3 (JCPDS card No. 04-006-2232).

The crystallite size was calculated using Equation (1) from [14];

$$D = \frac{0.9\times\lambda}{\beta\times\cos\theta} \quad (1)$$

Where D is the crystallite size, λ is the wavelength of the radiation, β is the FWHM in radians and θ is the Bragg's angle.

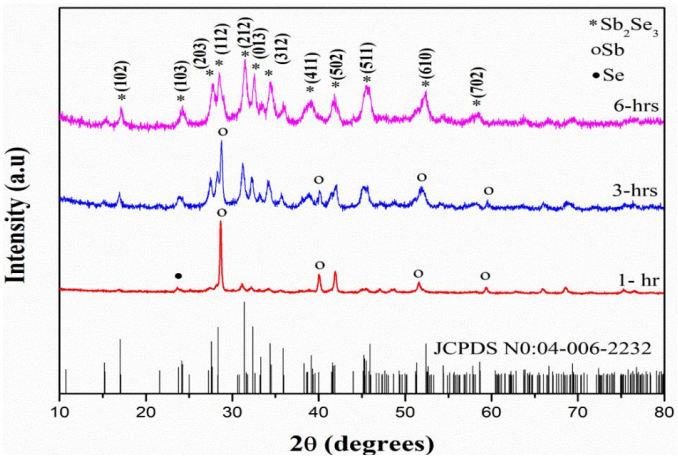

Fig-1: XRD pattern of as-milled (dry) Sb_2Se_3

Further analysis for phase formation in the as-milled Sb_2Se_3 was done by Raman spectroscopy studies. Raman spectroscopy is a non-destructive characterization technique with minimal sample requirement. The peak positions or Raman shift in the collected spectra gives information about the corresponding phase, whereas the shape of the peak and intensity indicates crystalline nature of the sample. Raman spectrum of the dry as-milled Sb_2Se_3 powder is shown in Figure 2. Raman shift of Sb_2Se_3 phase at 188 and 252 cm^{-1} were observed. The Raman spectra of Sb_2Se_3 indicate that it is of single phase with no secondary phases. Similar results were also reported by [3].

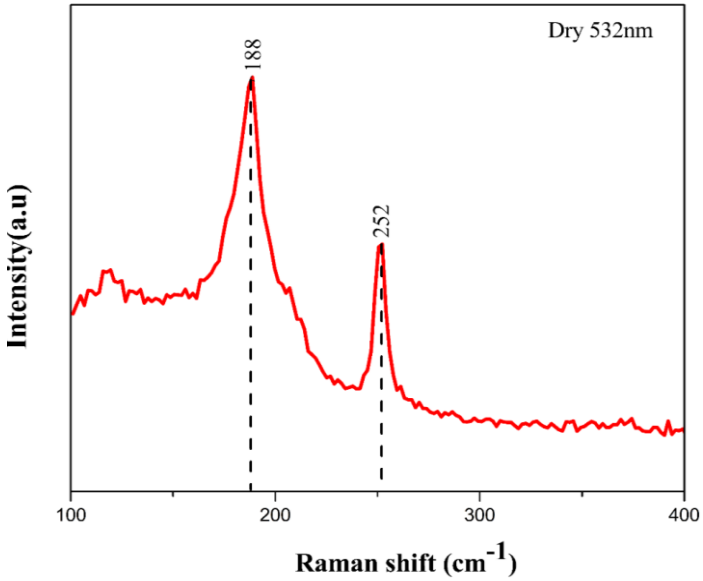

Fig-2: Raman Spectra dry milled Sb_2Se_3 (6 hours of dry milling)

Figure 3 displays the SEM image of the dry milled (6 hours) sample. The figure appears cloudy with large grains of the agglomerated powder particles.

EDAX spectrum shows the presence of antimony and selenium in sample.

Elemental composition analysis of the mass% and atom% of Antimony Selenide films are tabulated in Table 1.

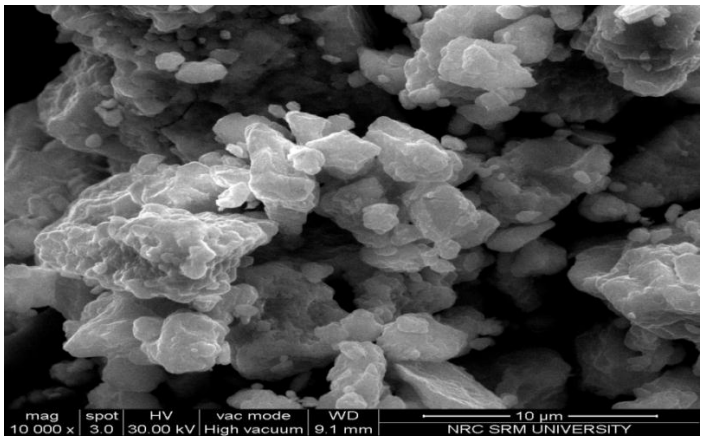

Fig-3: FE-SEM micrographs of the dry milled (6 hours) sample

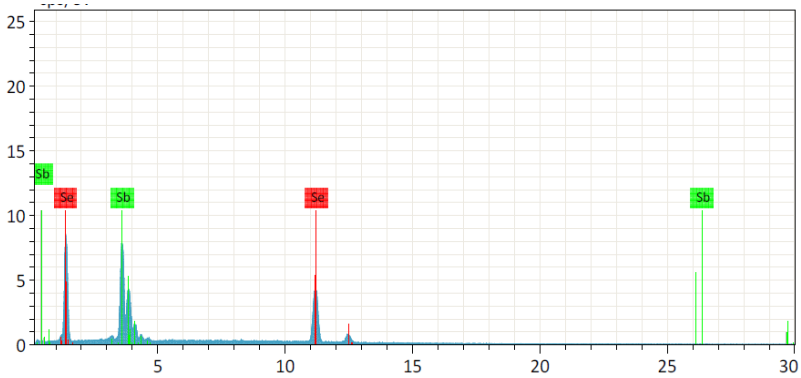

Fig-4: Elemental composition of the wet milled sample

Table-1: Elemental composition of the dry milled sample

Element	Mass%	Atomic%	Abs. error (%)	Rel. error (%)
Sb	54.63	43.85	1.61	3.00
Se	45.37	56.15	1.14	2.57
Sum	100.00	100.00	2.75	5.57

CONCLUSION

Using ball milling technique (dry), we have demonstrated the synthesis Sb_2Se_3 from Sb and Se powders. XRD, Raman, SEM and EDAX have shown that single phase Sb_2Se_3 can be achieved after 6 hours of milling.

REFERENCES

1. Zeng K, Xue DJ, Tang J. Antimony selenide thin-film solar cells. Semiconductor Science and Technology. 2016 Apr 19;31(6):063001.
2. Wang X, Tang R, Wu C, Zhu C, Chen T. Development of antimony sulfide–selenide Sb2 (S, Se) 3-based solar cells. Journal of energy chemistry. 2017 Oct 12.
3. Tiwari KJ, Ren MQ, Vajandar SK, Osipowicz T, Subrahmanyam A, Malar P. Mechanochemical bulk synthesis and e-beam growth of thin films of Sb 2 Se 3 photovoltaic absorber. Solar Energy. 2018 Jan 15;160:56-63.
4. Chen C, Li W, Zhou Y, Chen C, Luo M, Liu X, Zeng K, Yang B, Zhang C, Han J, Tang J. Optical properties of amorphous and polycrystalline Sb2Se3 thin films prepared by thermal evaporation. Applied Physics Letters. 2015 Jul 27;107(4):043905.
5. Ugwu EI. Optimized Theoretical Analysis of Antimony Selenide (Sb 2 Se 3) Chalcogenide Thin Film. InPIERS Proceedings 2014 Aug 25.
6. Ma J, Wang Y, Wang Y, Chen Q, Lian J, Zheng W. Controlled synthesis of one-dimensional Sb2Se3 nanostructures and their electrochemical properties. The Journal of Physical Chemistry C. 2009 Jul 2;113(31):13588-92.
7. Vadapoo R, Krishnan S, Yilmaz H, Marin C. Electronic structure of antimony selenide (Sb2Se3) from GW calculations. physica status solidi (b). 2011 Mar;248(3):700-5.
8. Mehta RJ, Karthik C, Jiang W, Singh B, Shi Y, Siegel RW, Borca-Tasciuc T, Ramanath G. High electrical conductivity antimony selenide nanocrystals and assemblies. Nano letters. 2010 Oct 6;10(11):4417-22.
9. Shen J, Blachnik R. Mechanochemical syntheses of antimony selenide, tin selenides and two tin antimony selenides. Thermochimica acta. 2003 Mar 24;399(1-2):245-6.
10. Yang J, Liu YC, Lin HM, Chen CC. A chain-structure nanotube: growth and characterization of single-crystal Sb2S3 nanotubes via a chemical vapor transport reaction. Advanced Materials. 2004 Apr 19;16(8):713-6.
11. Park KH, Choi J, Kim HJ, Lee JB, Son SU. Synthesis of antimony sulfide nanotubes with ultrathin walls via gradual aspect ratio control of nanoribbons. Chemistry of materials. 2007 Aug 7;19(16):3861-3.
12. Deng Z, Mansuripur M, Muscat AJ. Simple colloidal synthesis of single-crystal Sb− Se− S nanotubes with composition dependent band-gap energy in the near-infrared. Nano letters. 2009 Apr 24;9(5):2015-20.
13. Maghraoui-Meherzi H, Nasr TB, Dachraoui M. Synthesis, structure and optical properties of Sb2Se3. Materials Science in Semiconductor Processing. 2013 Feb 1;16(1):179-84.
14. Rajendran, V; Anitha, R; Dhanalakshmi, R and Vijayalakshmi, R (). Synthesis and characterisation of Antimony Selenide thin film. 2018; 5(7).
15. Zakaria Z, Chelvanathan P, Rashid MJ, Akhtaruzzaman M, Alam MM, Al-Othman ZA, Alamoud A, Sopian K, Amin N. Effects of sulfurization temperature on Cu2ZnSnS4 thin film deposited by single source thermal evaporation method. Japanese Journal of Applied Physics. 2015 Jul 27;54(8S1):08KC18.
16. Tiwari KJ, Kumar DP, Mallik RC, Malar P. Ball Mill Synthesis of Bulk Quaternary Cu 2 ZnSnSe 4 and Thermoelectric Studies. Journal of Electronic Materials. 2017 Jan 1;46(1):30-9.
17. Ota J, Srivastava SK. Synthesis and optical properties of Sb2Se3 nanorods. Optical Materials. 2010 Sep 1;32(11):1488-92.